Intra- and Intersubunit Cooperativity in Activation of BK Channels by Ca^{2+}

Xiang Qian, Xiaowei Niu, and Karl L. Magleby

Department of Physiology and Biophysics, University of Miami Miller School of Medicine, Miami, FL 33101

The activation of BK channels by Ca^{2+} is highly cooperative, with small changes in intracellular Ca^{2+} concentration having large effects on open probability (*Po*). Here we examine the mechanism of cooperative activation of BK channels by Ca^{2+}. Each of the four subunits of BK channels has a large intracellular COOH terminus with two different high-affinity Ca^{2+} sensors: an RCK1 sensor (D362/D367) located on the RCK1 (regulator of conductance of K^+) domain and a Ca-bowl sensor located on or after the RCK2 domain. To determine interactions among these Ca^{2+} sensors, we examine channels with eight different configurations of functional high-affinity Ca^{2+} sensors on the four subunits. We find that the RCK1 sensor and Ca bowl contribute about equally to Ca^{2+} activation of the channel when there is only one high-affinity Ca^{2+} sensor per subunit. We also find that an RCK1 sensor and a Ca bowl on the same subunit are much more effective in increasing *Po* than when they are on different subunits, indicating positive intrasubunit cooperativity. If it is assumed that BK channels have a gating ring similar to MthK channels with alternating RCK1 and RCK2 domains and that the Ca^{2+} sensors act at the flexible (rather than fixed) interfaces between RCK domains, then a comparison of the distribution of Ca^{2+} sensors with the observed responses suggest that the interface between RCK1 and RCK2 domains on the same subunit is flexible. On this basis, intrasubunit cooperativity arises because two high-affinity Ca^{2+} sensors acting across a flexible interface are more effective in opening the channel than when acting at separate interfaces. An allosteric model incorporating intrasubunit cooperativity nested within intersubunit cooperativity could approximate the *Po* vs. Ca^{2+} response for eight possible subunit configurations of the high-affinity Ca^{2+} sensors as well as for three additional configurations from a previous study.

The Journal of General Physiology

INTRODUCTION

Large conductance Ca^{2+}-activated K^+ (BK) channels are activated in a synergistic manner by intracellular Ca^{2+} (Ca^{2+}_i) and depolarization (Barrett et al., 1982; Kaczorowski et al., 1996; Magleby, 2003). When opened, the efflux of K^+ out of cells through the channels drives the membrane potential in the negative direction, which reduces excitability, shutting down Na^+ and Ca^{2+} channels. By coupling membrane potential and Ca^{2+}_i to excitability, BK channels modulate many processes, such as the contraction of smooth muscle and neurotransmitter release (Robitaille et al., 1993; Brenner et al., 2000; Petkov et al., 2001; Wang et al., 2001; Xu and Slaughter, 2005). Crucial in this coupling is the highly cooperative activation of BK channels by Ca^{2+}_i that allows small changes in Ca^{2+}_i to elicit large changes in open probability (*Po*), with Hill coefficients of typically 2–5 (Barrett et al., 1982; McManus et al., 1985; Golowasch et al., 1986; Cui et al., 1997; Nimigean and Magleby, 1999; Bian et al., 2001). In spite of its importance, the mechanism underlying the cooperative activation of BK channels by Ca^{2+}_i remains unclear.

The high Hill coefficients of BK channels suggest that a minimum of 2–5 Ca^{2+} must bind to the channel for full activation (Barrett et al., 1982; McManus et al., 1985; Golowasch et al., 1986; Cui et al., 1997; Nimigean and Magleby, 1999; Bian et al., 2001). Consistent with a large number of Ca^{2+} binding sites, BK channels are tetramers (Shen et al., 1994), and studies have suggested at least three different types of Ca^{2+} sensors per subunit (for review see Magleby, 2003). These sensors are associated with the large intracellular COOH terminus of the channel, which is thought to form a Ca^{2+}-activated gating ring comprised of eight RCK (regulators of the conductance of potassium) domains, two per subunit, designated RCK1 and RCK2 (Jiang et al., 2001, 2002; Niu et al., 2004). Two of the Ca^{2+} sensors are of high affinity (μM) and are defined by mutations to the Ca bowl and to D362/D367 (Schreiber and Salkoff, 1997; Schreiber et al., 1999; Xia et al., 2002; Zeng et al., 2005). The Ca^{2+} sensor silenced by the double mutation D362A/D367A will be referred to as the RCK1 sensor, since it is located on the RCK1 domain. Mutations to M513 may define the same high-affinity Ca^{2+} sensor

Correspondence to Xiang Qian: xiang.qian@ucsf.edu; or Karl Magleby: kmagleby@miami.edu

Xiang Qian's present address is Howard Hughes Medical Institute and Departments of Physiology and Biochemistry, University of California, San Francisco, CA 94143.

Abbreviations used in this paper: BK channel, large conductance Ca^{2+}- and voltage-activated K^+ channel; Ca^{2+}_i, intracellular Ca^{2+}; RCK, regulator of the conductance of potassium; WT, wild-type.

as mutations to D362/D367 (Bao et al., 2002). The third Ca^{2+} sensor is low affinity (mM), binds Ca^{2+} and Mg^{2+}, and is removed by mutations to E374/E399 (Shi and Cui, 2001; Zhang et al., 2001; Shi et al., 2002; Qian and Magleby, 2003). Under physiological conditions the low-affinity sensor would normally be occupied by Mg^{2+}. Low concentrations of Ca^{2+} that maximally activate the two types of high-affinity sensors have little effect on the low-affinity sensor (Shi and Cui, 2001; Zhang et al., 2001; Shi et al., 2002). Mutating all the Ca bowls or RCK1 sensors reduces the Ca^{2+} response about an equivalent amount, with the Ca bowl having a somewhat lower Kd. Joint mutations to the Ca bowl and D362/D367 or to the Ca bowl and M513 essentially eliminate all of the high-affinity Ca^{2+} sensitivity (Bao et al., 2002; Xia et al., 2002).

Because BK channels are tetrameric proteins, with each subunit containing two high-affinity Ca^{2+} sensors, several different mechanisms are possible for the cooperative activation of the channel by these sensors. (1) Each Ca^{2+} sensor, whether located on the same or different subunit, could be independent of all the other Ca^{2+} sensors, with the cooperativity in Ca^{2+} activation arising from the joint action of the independent Ca^{2+} sensors on opening the gates. (2) The two Ca^{2+} sensors on each subunit could interact, but act independently of the Ca^{2+} sensors on other subunits. (3) Ca^{2+} sensors on different subunits could interact but be independent of Ca^{2+} sensors on the same subunit. (4) All Ca^{2+} sensors, whether on the same or different subunits could interact. Interaction between Ca^{2+} sensors, either directly or allosterically, could lead to cooperativity through, for example, changing the Kd for Ca^{2+} binding. Combinations of the above cooperative mechanisms would also be possible. An assumption of independent Ca^{2+} sensors that act jointly to open the gates of the channel (option 1 above) is generally consistent with previous studies (Cox and Aldrich, 2000; Cui and Aldrich, 2000; Shi and Cui, 2001; Zhang et al., 2001; Horrigan and Aldrich, 2002; Niu and Magleby, 2002; Xia et al., 2002).

To test further the mechanism of cooperativity we now compare the Ca^{2+}-dependent activation of BK channels in which the high-affinity Ca^{2+} sensors on the gating ring are studied in different combinations on the same and different subunits. We find that channels with four high-affinity Ca^{2+} sensors distributed at one sensor per subunit were approximately equivalent in their ability for Ca^{2+} activation of the channel, independent of whether the four sensors were four RCK1 sensors, four Ca bowls, or two RCK1 sensors plus two Ca bowls. Thus, the two types of high-affinity Ca^{2+} sensors when distributed at one high-affinity Ca^{2+} sensor per subunit are approximately equivalent. It has previously been found that four RCK1 sensors are approximately equivalent to four Ca-bowl sensors (Bao et al., 2002; Xia et al., 2002). Our observations extend the equivalence to mixtures of the two types of high-affinity Ca^{2+} sensors, provided there is only one high-affinity sensor per subunit. In addition, we find that two high-affinity Ca^{2+} sensors located on the same subunit are much more effective in activating the channel than when located on different subunits, indicating positive intrasubunit cooperativity.

An extension of previous allosteric models (Cox and Aldrich, 2000; Cui and Aldrich, 2000; Shi and Cui, 2001; Zhang et al., 2001; Xia et al., 2002; Niu and Magleby, 2002) to incorporate intrasubunit cooperativity in which high-affinity Ca^{2+} sensors on the same subunit are more effective than when on separate subunits could approximate the *Po* vs. Ca^{2+} response for eight possible subunit configurations of the high-affinity Ca^{2+} sensors as well as three additional configurations from a previous study. In this extended model the intrasubunit cooperativity is nested within the intersubunit cooperativity. If it is assumed by analogy to MthK channels (Jiang et al., 2002) (a) that BK channels have a gating ring comprised of eight RCK domains that are separated by alternating fixed and flexible interfaces, and (b) that the Ca^{2+} sensors must work at a flexible interface, then a comparison of the possible configurations of the Ca^{2+} sensors on the subunits of BK channels in our experiments with the observed Ca^{2+} responses suggests that the flexible interfaces are intrasubunit and the fixed interfaces are intersubunit. On this basis, intrasubunit cooperativity arises because a pair of high-affinity Ca^{2+} sensors working across a flexible interface within a subunit gives a greater shift in the equilibrium toward the open state than when the sensors act separately on separate subunits.

MATERIALS AND METHODS

Clones, Mutagenesis, and Channel Expression

Experiments were performed using the mouse Slo1 α subunit of the BK channel provided by Merck Research Laboratories. This subunit was initially cloned by Pallanck and Ganetzky (1994), GenBank/EMBL/DDBJ accession no. U09383, before modification by Merck Research Laboratories (McManus et al., 1995). Alpha subunits with mutations to the Ca^{2+} sensors in the Ca bowl (5D5N mutant: FLDQDDDDDPD to FLDQNNNNNPD) and in the RCK1 sensor (D362A/D367A mutant: FLKDFLHKDRDD to FLKAFLHKARDD), and with mutations of both 5D5N and D362A/D367A were provided by X. Xia and C. Lingle (Washington University School of Medicine, St. Louis, MO) (Xia et al., 2002). Using these constructs, we made two additional mutant subunits that were insensitive to block by extracellular TEA by mutating a site in the pore region of the channel (Y294V: GYGDVYAKT to GYGDVVAKT), as described previously (Niu and Magleby, 2002) to obtain Y294V/5D5N and Y294V/5D5N/D362A/D367A mutant subunits. (The numbering differs from our previous paper [Niu and Magleby, 2002] because the counting starts 40 amino acids later at the second methionine.) Mutations were made by using Stratagene's QuikChange Site-Directed Mutagenesis Kit and were checked by sequencing. The cDNA was transcribed in vitro by using the mMESSAGE mMACHINE Kit (Ambion) to obtain cRNA for injection into *Xenopus* oocytes. Oocytes were microinjected with 0.5–20 ng of cRNA 2–8 d before

recording. When expressing channels with two different types of subunits, the cRNA was injected in a 1:1 ratio.

Electrophysiology and Solutions

Single-channel currents were recorded with the patch clamp technique (Hamill et al., 1981) from inside-out patches of membrane excised from *Xenopus* oocytes using an Axopatch 200B amplifier (Axon Instruments, Inc.). The pipette solution contained 158 mM KCl and 5 mM *N*-[tris(hydroxymethyl)methyl]-2-aminoethanesulfonic acid (TES) pH buffer. The bath solution contained 158 mM KCl, 5 mM TES, 1 mM EGTA, 1 mM *N*-(2-hydroxyethyl) ethylenediamine-*N*,*N*′,*N*′-triacetic acid (HEDTA), and sufficient added $CaCl_2$ to obtain the desired free Ca^{2+} concentrations of 1–1,000 μM. All solutions were adjusted to pH 7.0. Solutions with a calculated free Ca^{2+} of $\leq 10^{-8}$ M will be referred to as 0 Ca^{2+} solutions because $Ca^{2+}{}_i$ at these concentrations has essentially no effect on the gating of the channel (Nimigean and Magleby, 2000). Voltages refer to the intracellular potential. Experiments were performed at room temperature (20–23°C).

Data Analysis

Single-channel data were sampled at 200 kHz and typically filtered to 2–5 kHz using pClamp8 or pClamp9 (Axon Instruments, Inc.). Analysis of the digitized records was then performed using custom programs and Clampfit 9.0 (Axon Instruments, Inc.), as described previously (McManus et al., 1987; McManus and Magleby, 1988; Nimigean and Magleby, 1999). Fitting of equations to the *Po* vs. $Ca^{2+}{}_i$ plots was accomplished with the nonlinear least squares fitting routines in SigmaPlot 2000 (Systat Software Inc.). Data are expressed as the mean ± SEM.

RESULTS

Two Different High-affinity Ca^{2+} Sensors Contribute to the Cooperative Activation of BK Channels by $Ca^{2+}{}_i$

To investigate the mechanism for cooperative activation of BK channels by $Ca^{2+}{}_i$, we constructed and identified modified BK channels with different configurations of the high-affinity Ca^{2+} sensors on the subunits. Fig. 1 A presents a cartoon of a single α subunit from a wild type (WT) BK channel. Similar to the super family of voltage-activated channels, the α subunit contains transmembrane segments S1–S6, including a positively charged S4 domain that functions as a voltage sensor (Atkinson et al., 1991; Adelman et al., 1992; Butler et al., 1993; Diaz et al., 1998; Cui and Aldrich, 2000), and a P-loop to form the selectivity filter of the channel (Doyle et al., 1998). In addition, BK channels have an S0 domain that places the NH_2 terminus extracellular (Meera et al., 1997) and a large intracellular COOH terminus that has two high-affinity Ca^{2+} sensors: the Ca bowl located at the end of the RCK2 domain near the end of the COOH terminus (Schreiber and Salkoff, 1997) and a Ca^{2+} sensor defined by the mutation D362A/D367A (to be referred to as the RCK1 sensor) located upstream of the Ca bowl in the RCK1 domain of the COOH terminus (Xia et al., 2002). The schematic notation used to represent the tetrameric structure of the WT channel with its eight high-affinity Ca^{2+} sensors, two per subunit, is also shown in Fig. 1 A, where the blue squares are RCK1 sensors (R) and the red hexagons are Ca bowls (B). The alphanumeric notation for WT channels is then 4(RB), indicating that each of the four subunits have an RCK1 sensor (R) and a Ca bowl (B). When RCK1 sensors or Ca bowls are eliminated by mutation, the sensor designation letter is replaced with a Δ.

The WT channel with its two high-affinity Ca^{2+} sensors per subunit is fully activated by 100 μM Ca^{2+} at +50 mV, giving an open probability (*Po*) of >0.9, as shown by the upper single-channel current record in Fig. 1 A. After reducing the number of high-affinity Ca^{2+} sensors per subunit from two to one by mutating either the RCK1 sensor (Fig. 1 B, 4(ΔB)), or the Ca bowl (Fig. 1 C, 4(RΔ)), 100 μM $Ca^{2+}{}_i$ only partially activated the channel, giving average *Po*s for the channels in these experiments of ∼0.40 and ∼0.35, respectively (Fig. 1, B and C, top traces are excerpts from longer records).

When both high-affinity Ca^{2+} sensors on each subunit were removed by mutation, producing 4(ΔΔ) channels, then 100 μM Ca^{2+} had little effect on channel activity, giving a *Po* of <0.01, (Fig. 1 D, top trace). Results from a series of experiments over a range $Ca^{2+}{}_i$ for the four types of modified channels shown in Fig. 1, WT 4(RB), 4(ΔB), 4(RΔ), and 4(ΔΔ), are presented in Fig. 2 together with data from a another type of modified channel, 2(ΔB)+2(RΔ), to be discussed later. The curves are fits with the Hill function,

$$Po = \frac{P_{\max}}{1 + (K_d / [Ca^{2+}{}_i])^n}, \quad (1)$$

where $P_{\max}$ is the maximum *Po*, 0.92, K_d is an apparent K_d indicating the $Ca^{2+}{}_i$ required for half activation, and n is the Hill coefficient that reflects the slope of the dose–response relationship. Because the response from the 4(ΔB) channels, the 4(RΔ) channels, and the 2(ΔB)+2(RΔ) channels (to be discussed later) was similar, the data from these three types of channels were fitted with a single curve. The K_d for WT channels was 2.01 μM with a Hill coefficient of 3.30 (dashed line) compared with a K_d of ∼94.4 μM and a Hill coefficient of ∼1.05 for the 4(ΔB), 4(RΔ), and 2(ΔB)+2(RΔ) channels (continuous line). Thus, removing either the four Ca bowls (plotted blue squares) or the four RCK1 sensors (plotted red hexagons) shifted the K_d to the right by ∼92 μM and decreased the Hill coefficient by ∼2.2. The similar response for 4(ΔB) channels and 4(RΔ) channels in Fig. 2 indicates that four RCK1 sensors or four Ca bowls are about equally effective in activating the channel. Removing all eight of the high-affinity Ca^{2+} sensors to obtain 4(ΔΔ) channels removed all of the Ca^{2+} sensitivity up to ∼1,000 μM (green triangles). Thus, RCK1 sensors or Ca bowls are required for the channel to detect micromolar concentrations of $Ca^{2+}{}_i$. The small response with $Ca^{2+}{}_i$ >1000 μM for the 4(ΔΔ)

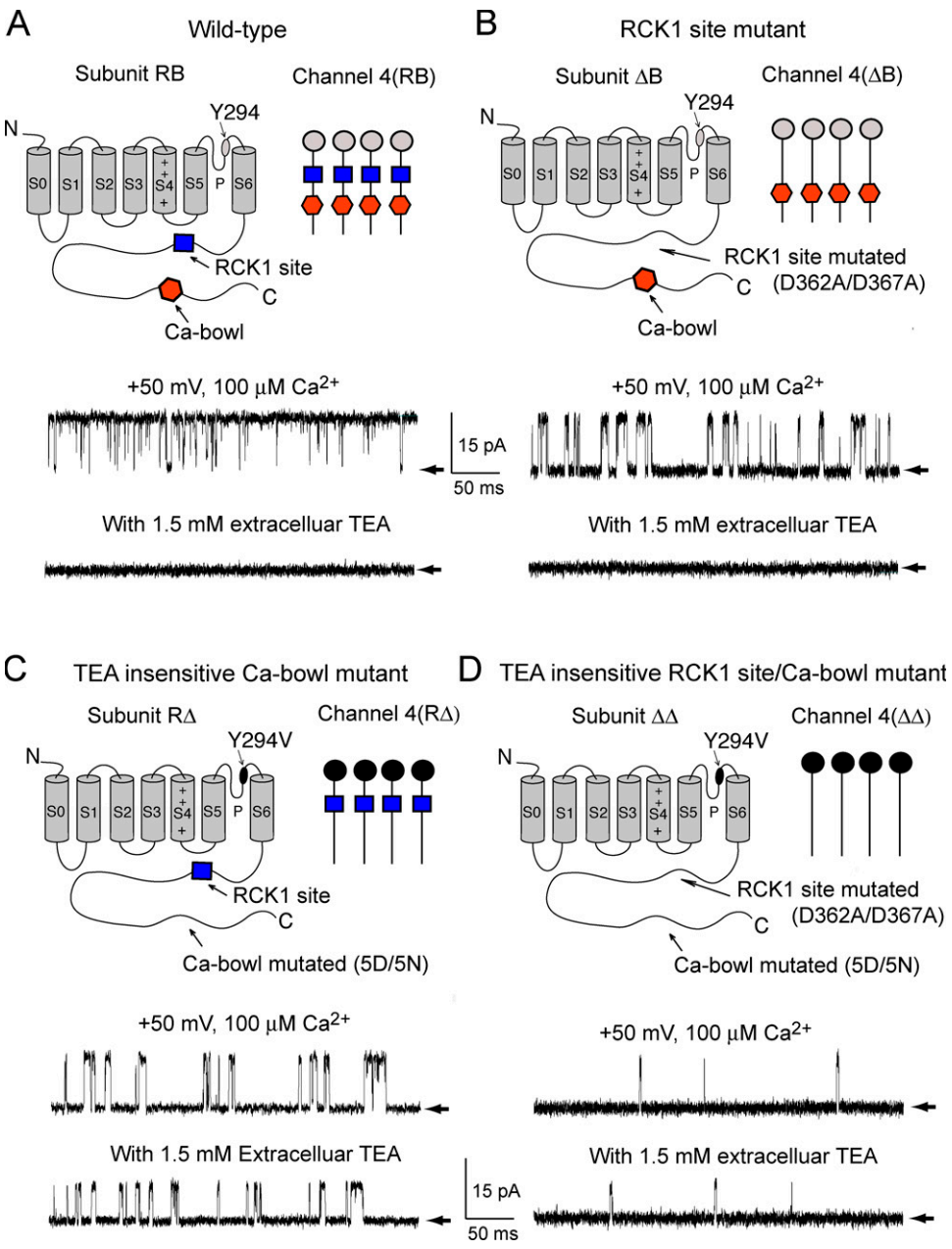

Figure 1. Structure and function of four homotetrameric configurations of high-affinity Ca^{2+} sensors used to investigate cooperativity among Ca^{2+} sensors. (A) Cartoon of a single WT subunit (upper left) and a schematic diagram of a WT channel formed from four of these subunits (upper right). Each WT subunit has two high-affinity Ca^{2+} sensors on the intracellular COOH terminus, an RCK1 sensor (R) and a Ca-bowl sensor (B), giving an (RB) subunit. WT channels are comprised from four such subunits, designated 4(RB). WT channels were fully activated with 100 μM $Ca^{2+}{}_i$ at + 50 mV, as indicated by the single-channel current record (upper current trace). Addition of 1.5 mM extracellular TEA, (TEA_O) completely blocked the currents (lower trace). Arrows indicate the closed current level. (B) Mutation of the RCK1 site produces a ΔB subunit, where Δ indicates a mutated sensor. Homomeric 4(ΔB) channels expressed from ΔB subunits have greatly reduced activation with 100 μM $Ca^{2+}{}_i$ (upper current trace) and can be blocked by 1.5 mM TEA_O. (C) Mutation of the Ca-bowl site produces an RΔ subunit. Homomeric 4(RΔ) channels expressed from RΔ subunits also have greatly reduced activation with 100 μM $Ca^{2+}{}_i$. The channel is not blocked by TEA_O because of the presence of a Y294V pore mutation (lower trace). (D) Mutation of both the RCK1 sensor and the Ca bowl produce ΔΔ subunits. Homomeric 4(ΔΔ) channels are Ca^{2+} insensitive up to 1,000 μM Ca^{2+}. The channel is not blocked by TEA_O because of the presence of a Y294V pore mutation (lower trace). Current traces in this and the following figures are representative excerpts from longer records.

channels reflects a separate low-affinity Ca^{2+}/Mg^{2+} sensor (Shi and Cui, 2001; Zhang et al., 2001; Xia et al., 2002; Shi et al., 2002). These single-channel observations on the contributions of four Ca-bowl sensors, four RCK1 sensors, and four low-affinity sensors to the Ca^{2+} activation of the channel are generally consistent with previous studies using macroscopic recordings (Bao et al., 2002; Xia et al., 2002).

Cooperativity in channel activation is readily apparent in Fig. 2. For example, with either four RCK1 sensors or four Ca bowls, the *Po* was ~0.1 with 13 μM $Ca^{2+}{}_i$ (continuous line). With both four Ca bowls and four RCK1 sensors, as is the case for the WT channels, the *Po* for the same $Ca^{2+}{}_i$ was >0.9, and the *Po* vs. $Ca^{2+}{}_i$ response was much steeper (dashed line). Hence, rather than a doubling of *Po*, as might occur if the responses were additive, there was a ninefold increase in response.

Expressing and Identifying Channels with Different Subunit Distributions of the Two High-affinity Ca^{2+} Sensors

To determine whether the greatly enhanced response when both the RCK1 sensors and Ca bowls were present might arise from interactions of these two types of high-affinity Ca^{2+} sensors within or between subunits, we studied channels constructed with a total of four high-affinity sensors distributed to either facilitate

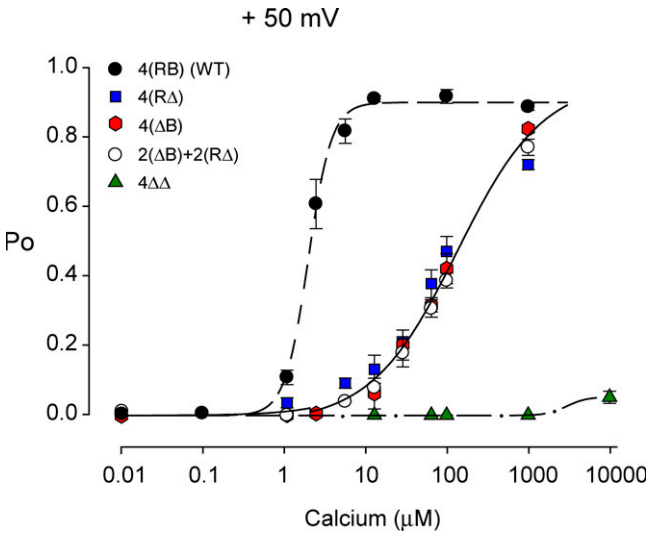

Figure 2. RCK1 sensors and Ca bowls are approximately equivalent in activating BK channels when distributed on separate subunits. *Po* vs. Ca^{2+}_i plots for 4(RB), 4(RΔ), 4(ΔB), 2(ΔB)+2(RΔ), and 4(ΔΔ) channels. Data for each plotted point is from 5–7 single-channel patches. The lines are fits with the Hill equation (Eq. 1). The data from the 4(RΔ), 4(ΔB), and 2(ΔB)+2(RΔ) channels cluster together, and consequently these data were simultaneously fit to obtain the continuous line through the data. The K_d for the 4(RB) and combined 4(RΔ), 4(ΔB), and 2(ΔB)+2(RΔ) channels are 2.01 and 94.4 μM, respectively, with Hill coefficients of 3.30 and 1.05, respectively. In this and the following figures data that were obtained for a free $Ca^{2+} \leq 0.01$ μM are plotted at 0.01 μM to save space, as there was no difference in response at such low Ca^{2+}. Points at 0.01 have been displaced slightly so they can be seen.

intrasubunit interactions, 2(RB)+2(ΔΔ), or intersubunit interactions, 2(ΔB)+2(RΔ). Schematic diagrams of the subunit composition of these channels are shown in Fig. 3 A, together with diagrams for the other channels examined in this paper. The 2(RB)+2(ΔΔ) channels would facilitate exploration of intrasubunit interactions of the Ca^{2+} sensors because two of the subunits have two high-affinity Ca^{2+} sensors on the same subunit and the other two subunits have no high-affinity Ca^{2+} sensors. The 2(ΔB)+2(RΔ) channels would facilitate exploration of intersubunit interactions because each subunit has only one high-affinity Ca^{2+} sensor per subunit. The fact that each of these channel types has two RCK1 sensors and two Ca bowls facilitates comparison of the results. Because it is not known whether there would be a preferential assembly of the two types of subunits in each channel either adjacent or diagonal to one another, both types of assembly are shown in Fig. 3 A.

Because the NH_2 terminus of the α subunit is located extracellularly and the COOH terminus intracellularly, it is not possible to construct directly tandem 2(RB)+2(ΔΔ) or tandem 2(ΔB)+2(RΔ) channels. To overcome this limitation, we coexpressed the required subunits and identified the subunit composition of each studied single channel by using a mutation in the outer pore region of specific subunits to change the channel's sensitivity to be blocked by extracellular TEA, TEAo (Shen et al., 1994; Niu and Magleby, 2002; Tian et al., 2004). Because the reduction in single-channel current amplitude is approximately proportional to the number of subunits with the TEA blocking site intact, it is possible to determine the subunit composition for channels formed from two different coexpressed subunits, provided that one of the two subunit types has the TEA site mutation. In the schematic diagrams, the channels with the TEA site intact are gray and the channels with the TEA site mutated are black. Fig. 1 (A and B, bottom traces) shows that channels comprised of four subunits in which the tyrosine residue Y294 on each subunit in the outer pore region of the channel was intact were fully blocked by 1.5 mM TEAo for WT and 4(ΔB) channels, respectively. In contrast, 1.5 mM TEAo gave only a small reduction in current when the TEA binding site on all four subunits was changed to valine (Fig. 1, C and D, bottom traces) for 4(RΔ) and 4(ΔΔ) channels, respectively.

To obtain 2(RB)+2(ΔΔ) channels, we coexpressed WT (RB) subunits (homomeric response in Fig. 1 A) with (ΔΔ) subunits in which the RCK1 sensor, the Ca bowl, and the TEA blocking site were all mutated (homomeric response in Fig. 1 D). In the absence of TEAo, all of the channels from this coexpression had the same current level of ~13.0 pA. In the presence of 1.5 mM TEAo, the current amplitudes from different channels could be different, but the response from any single channel remained constant (Fig. 3 B). Responses from 20 patches indicated four different levels of unitary current amplitude: 2.0, 4.3, 7.5, and 9.4 pA (Fig. 3 C), with the zero current level coming from experiments like that in Fig. 1 A. Because single-channel current amplitudes increase with the number of subunits that have mutated TEA binding sites (Shen et al., 1994; Niu and Magleby, 2002; Tian et al., 2004), the subunit composition of the channel can be deduced, as indicated in Fig. 3 B, where current amplitudes of ~4–5 pA indicate 2(RB)+2(ΔΔ) channels. The same approach was used to obtain 2(ΔB)+2(RΔ) channels. ΔB subunits (homomeric response in Fig. 1 B) were coexpressed with (RΔ) subunits (homomeric response in Fig. 1 C), and the 2(ΔB)+2(RΔ) channels were then indicated by a current level of ~5 pA (Fig. 3 E). Previous studies have shown that the *Po* of BK channels is not affected by mutations to the TEA sites (Niu and Magleby, 2002) or by the presence of TEA_O (Langton et al., 1991). We have also observed for inside-out patches that WT channels in the absence of TEA_O have a *Po* vs. Ca^{2+} response similar to channels in the presence of 1.5 mM TEA_O expressed from a combination of WT subunits and subunits with the TEA site mutated. In some experiments that were carried out with outside-out patches so

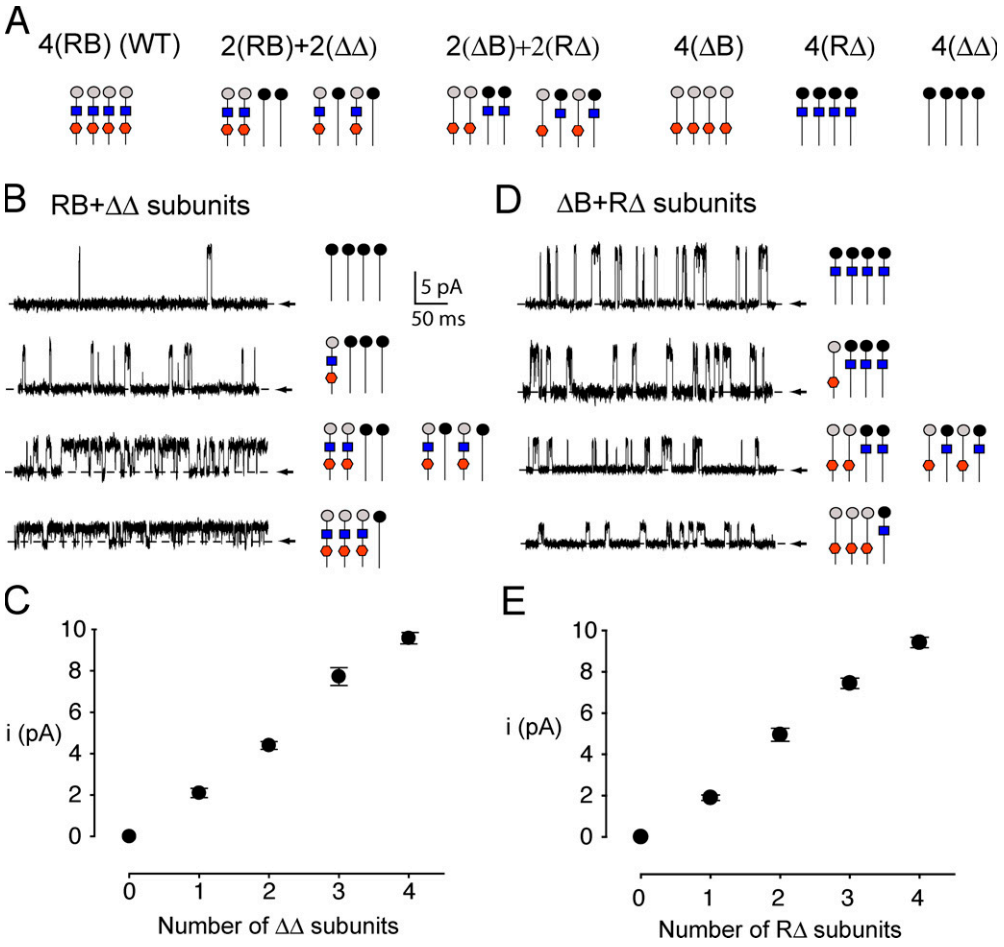

Figure 3. Identification of the subunit stoichiometry of the heteromeric channels used to explore intrasubunit cooperativity. (A) Presentation of the channels examined in this study, their channel designation, and distributions of the high-affinity Ca^{2+} sensors on the subunits, where blue squares are RCK1 sensors and red hexagons are Ca bowls. For 2(RB)+2(ΔΔ) and 2(ΔB)+2(RΔ) channels, both adjacent and diagonal subunit configurations are shown. (B) 2(RB)+2(ΔΔ) channels were obtained by coexpressing RB subunits together with ΔΔ subunits that had the Y294V pore mutation to relieve TEA_O block. Each expressed channel had one of five distinct current amplitudes in the presence of 1.5 mM TEA_O. Examples of single-channel currents (+50 mV) from channels with one of the four nonzero current amplitudes are presented. (An example of the zero current amplitude is presented in Fig. 1 A where the channel was first identified in the absence of TEA_O.) The deduced subunit stoichiometry for each of the current amplitudes is shown at the right, with both possible configurations for the 2(RB)+2(ΔΔ) channel shown. The 2(RB)+2(ΔΔ) channel can be identified by a current level of ∼5 pA at + 50 mV. (C) Plot of single-channel current amplitude against the number of ΔΔ subunits, assuming that the current amplitude is proportional to the number of subunits with the pore site mutation that removes TEA_O block. (D and E) 2(ΔB)+2(RΔ) channels were obtained by coexpressing (ΔB) subunits together with RΔ subunits that had the Y294V pore mutation that relieved TEA_O block. 2(ΔB)+2(RΔ) channels were identified by a current level of ∼5 pA at + 50 mV, following the same strategy as used above.

that the extracellular solution could be changed, a small TEA_O-induced decrease in *Po* (∼5 mV right shift of the *Po-V* curve) could be observed (to be presented elsewhere). Why TEA_O appears to have a small effect in some studies and little or no effect in others is unclear. Nevertheless, all these observations when taken together indicate that any possible effects of TEA_O on *Po* are expected to be small, suggesting that the assay system used to identify subunit composition of channels should be suitable for the needs of the present study.

4(RΔ), 4(ΔB), and 2(ΔB)+2(RΔ) Channels Have a Similar Ca^{2+} Response

The data in Figs. 1 and 2 showed a similar Ca^{2+} response for homomeric channels with four Ca bowls (4(ΔB) channels) or four RCK1 sensors (4(RΔ) channels). A common feature between these two types of channels is one high-affinity Ca^{2+} sensor per subunit. If the RCK1 sensors and Ca bowls are approximately equivalent in Ca^{2+} activation, as the data in Fig. 2 suggest, then heteromeric 2(ΔB)+2(RΔ) channels, which also have one high-affinity Ca^{2+} sensor per subunit, but a mixture of high-affinity sensors, should respond to Ca^{2+} the same as the homomeric 4(RΔ) channels and the homomeric 4(ΔB) channels. Using the methods outlined in Fig. 3 (D and E), we identified 2(ΔB)+ 2(RΔ) channels and plotted their response to Ca^{2+} in Fig. 2 (open circles). As indicated above, the Ca^{2+} response for 2(ΔB)+2(RΔ) channels was generally similar to that for 4(RΔ) channels and also for 4(ΔB) channels. Thus, the relative equivalence of RCK1 sensors and Ca bowls for Ca^{2+} activation extends to channels with a mixture of both types of high-affinity Ca^{2+} sensors, provided that there is only one high-affinity Ca^{2+} sensor per subunit.

From the differential distributions of high-affinity Ca^{2+} sensors on the subunits of the 4(ΔB), 4(RΔ), and 2(ΔB)+2(RΔ) channels (Fig. 3 A), it seems unlikely that the high-affinity Ca^{2+} sensors on these different

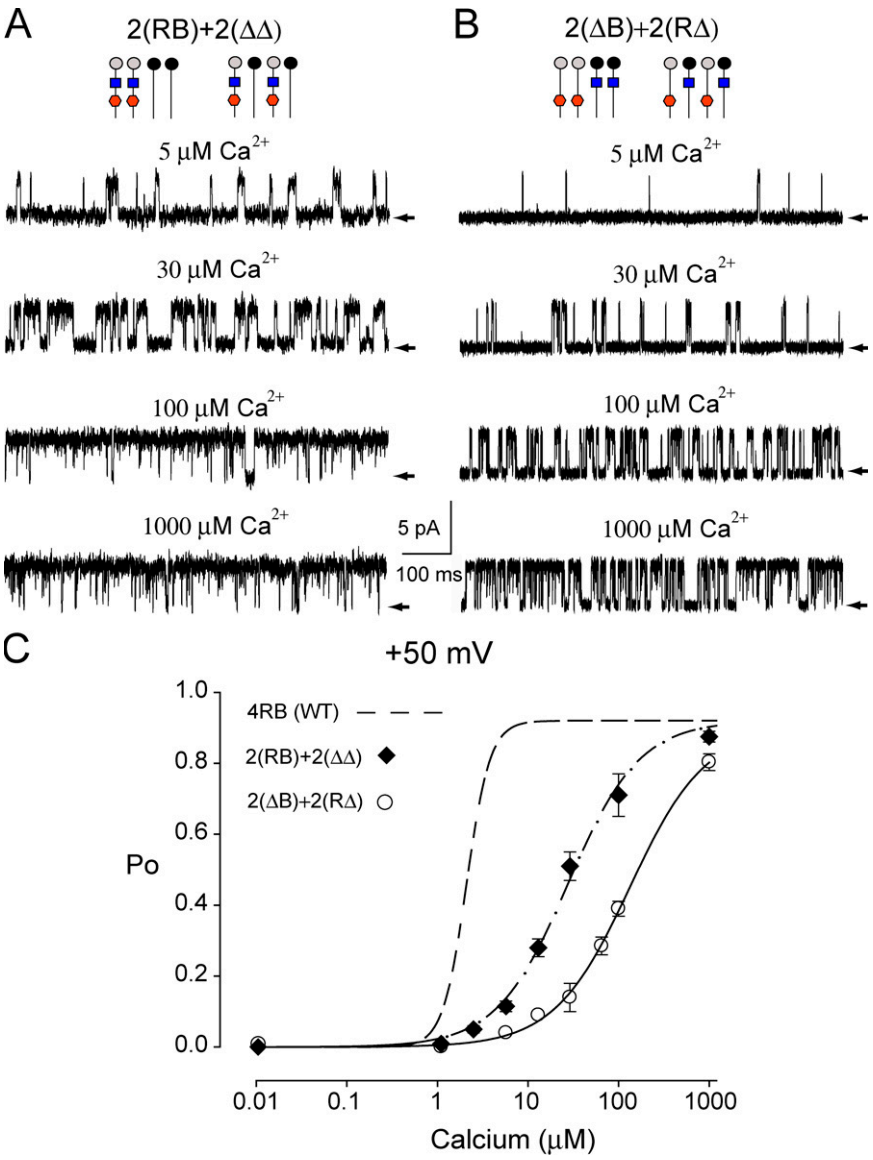

Figure 4. Two high-affinity Ca^{2+} sensors on the same subunit are more effective than when on different subunits, indicating intrasubunit cooperativity. (A and B) Representative single-channel currents recorded from a 2(RB)+2(ΔΔ) channel (A) and a 2(ΔB)+2(RΔ) channel (B) at four different Ca^{2+}_i at +50 mV. The *Po* is higher at each level of Ca^{2+}_i when two of the four subunits have two high-affinity Ca^2 sensors each, rather than when each of the four subunits has a single high-affinity Ca^{2+} sensor. TEA_O (1.5 mM) was present for both channels. (C) Plots of *Po* vs. Ca^{2+}_i for the indicated channel types: 2(RB)+2(ΔΔ) channels (filled diamonds, K_d = 29.7μM, Hill coefficient = 1.35) require less Ca^{2+}_i for the same *Po* than 2(ΔB)+2(RΔ) channels (open circles, K_d = 114.4 μM, Hill coefficient = 1.04). The dashed line is the response for WT channels from Fig. 2. Data for each plotted point is from 5–7 single-channel patches.

channels would directly interact with each other in a consistent manner for all three channels. Yet, these channels display similar responses to Ca^{2+}_i, suggesting that the high-affinity Ca^{2+} sensors on different subunits act relatively independently of one another.

High-affinity Ca^{2+} Sensors on the Same Subunit Display Intrasubunit Cooperativity

If high-affinity Ca^{2+} sensors always act independently of one another, then the Ca^{2+} response of the channel should depend only on the number of high-affinity Ca^{2+} sensors in the channel, independent of whether they are on the same or different subunits. To test for independence, we compared two different configurations of the high-affinity Ca^{2+} sensors, each with a total of four high-affinity Ca^{2+} sensors per channel, but distributed differently. For 2(RB)+2(ΔΔ) channels, two of the subunits have two high-affinity Ca^{2+} sensors each and the other two subunits have no high-affinity Ca^{2+} sensors. For 2(ΔB)+2(RΔ) channels, there is one high-affinity Ca^{2+} sensor for each subunit. Both of these channel types have two RCK1 sensors and two Ca bowls.

Representative single-channel currents recorded at four different Ca^{2+}_i for these two types of channels are shown in Fig. 4. For both channel types *Po* increased as Ca^{2+}_i was increased, but the *Po* was higher at each examined Ca^{2+}_i for 2(RB)+2(ΔΔ) channels (Fig. 4 A) than for 2(ΔB)+2(RΔ) channels (Fig. 4 B). Data from a series of experiments of this type are presented in Fig. 4 C as *Po* vs. Ca^{2+}_i plots. Clearly, four Ca^{2+} sensors distributed so that two of the subunits have two Ca^{2+} sensors each (as RCK1/Ca-bowl pairs) and two of the subunits have no Ca^{2+} sensors (2(RB)+2(ΔΔ) channels) gave a greater response to Ca^{2+} (filled diamonds) than when the same four Ca^{2+} sensors were distributed separately as one Ca^{2+} sensor per subunit (open circles, 2(ΔB)+2(RΔ) channels).

The K_d for the 2(RB)+2(ΔΔ) channels (29.7 μM) was 3.9-fold less than the K_d for 2(RΔ)+2(ΔB) channels (114.4 μM), with Hill coefficients of 1.35 and 1.04, respectively. For comparison, the response of the WT channel with its four pairs of RCK1/Ca-bowl Ca^{2+} sensors is indicated as a dashed line. The greater Ca^{2+} response for 2(RB)+2(ΔΔ) channels when compared with 2(RΔ)+2(ΔB) channels indicates a positive cooperativity in activation between the Ca bowl and the RCK1 sensor when they are located on the same subunit.

Both Adjacent and Diagonal Subunit Orientations of Identical Subunits are Likely to be Expressed for Both 2(RB)+2(ΔΔ) and 2(ΔB)+2(RΔ) Channels

Each of the heteromeric channels 2(ΔB)+2(RΔ) and 2(RB)+2(ΔΔ) examined for Fig. 4 can potentially assemble in two configurations: with identical subunits either adjacent or diagonal to one another, as diagrammed in Fig. 4 (A and B). Our observations that functional channels can be expressed with different numbers of high-affinity Ca^{2+} binding sites per subunit in a wide range of configurations with identical subunits either adjacent, diagonal, or both configurations (Figs. 1–4; Niu and Magleby, 2002) would suggest that there are no excluded assemblies of subunits with different configurations of Ca^{2+} sensors. Thus, both adjacent and diagonal distributions of identical subunits for both the 2(ΔB)+2(RΔ) and the 2(RB)+2(ΔΔ) channels are expected to be expressed. We could not directly test whether adjacent and diagonal configurations have similar responses to Ca^{2+}, but our observations that the observed variability in response, as indicated by the error bars in the *Po* vs. $Ca^{2+}{}_i$ plots (Fig. 4 C), was no greater for heteromeric than homomeric channels suggests, to a first approximation, that the Ca^{2+} response for channels with adjacent or diagonal identical subunits was similar.

Predicting the Ca^{2+} Response with Combined Intra- and Intersubunit Cooperativity

The Ca^{2+} activation of BK channels has been described by models with two high-affinity Ca^{2+} sensors and one low-affinity Ca^{2+}/Mg^{2+} sensor on each subunit. In these models the three types of Ca^{2+} sensors work independently of one another to control the gating, with the cooperativity in activation by $Ca^{2+}{}_i$ arising from the joint action of the three types of Ca^{2+} sensors on the opening–closing transitions, and not from interactions among the Ca^{2+} sensors (Cox et al., 1997; Cox and Aldrich, 2000; Shi and Cui, 2001; Zhang et al., 2001; Xia et al., 2002; Niu and Magleby, 2002; Hu et al., 2003). For a fixed voltage, these interactions can be described by

(SCHEME 1)

$$Po = \frac{P_{max}}{1 + L(V)\left(\frac{1+[Ca]/K_{RC}}{1+[Ca]/K_{RO}}\right)^{n1}\left(\frac{1+[Ca]/K_{BC}}{1+[Ca]/K_{BO}}\right)^{n2}\left(\frac{1+[Ca]/K_{MC}}{1+[Ca]/K_{MO}}\right)^{n3}},$$

where *Po* is the open probability, P_{max} is the maximum observed *Po*, K_{RC} and K_{RO} are the equilibrium constants for the binding of Ca^{2+} to the closed and open states of each high-affinity RCK1 site, K_{BC} and K_{BO} are the equilibrium constants for the binding of Ca^{2+} to the closed and open states of each high-affinity Ca bowl, K_{MC} and K_{MO} are the equilibrium constants for binding of Ca^{2+} to the closed and open states of each low-affinity Ca^{2+}/Mg^{2+} site, n_1, n_2, and n_3 are the number of RCK1 sensors, Ca bowls, and low-affinity sensors, respectively, each with a value of four in WT channels, and $L(V)$, with a value of 2,500 at +50 mV, is the allosteric gating factor that is determined directly in the absence of $Ca^{2+}{}_i$ (Cox et al., 1997; Niu and Magleby, 2002; Xia et al., 2002). In Scheme 1, the equilibrium constants do not change with the number of bound Ca^{2+}, indicating independent (noninteracting) $Ca2^{+}$ sensors. In addition, based on Scheme 1, the Ca^{2+} response of the channel should depend only on the number of Ca^{2+} sensors of each type in the channel, independent of whether they are on the same or different subunits.

However, as shown in Fig. 4, two high-affinity Ca^{2+} sensors on the same subunit are more effective in activating the channel than when on different subunits. Thus, the implicit assumption of independence between high-affinity Ca^{2+} sensors in Scheme 1 requires modification. To approach this problem, we examined whether an expanded model that includes positive cooperative interactions between RCK1 sensors and Ca bowls located on the same subunit can account for the data. This model is described by Scheme 2, where W is an empirical factor that indicates the intrasubunit cooperativity for RCK1 sensors and Ca bowls located on the same subunit, n_1 is the number of subunits with both a Ca bowl and an RCK1 sensor, n_2 is the number of subunits with an RCK1 sensor and without a Ca bowl, n_3 is the number of subunits without an RCK1 sensor and with a Ca bowl, and n_4 is the number of subunits with a low-affinity sensor. For WT channels, $n_1 = 4$, $n_2 = 0$, $n_3 = 0$, and $n_4 = 4$. For 2(RB)+2(ΔΔ) channels, $n_1 = 2$, $n_2 = 0$, $n_3 = 0$, and $n_4 = 4$. For 2(ΔB)+2(RΔ) channels, $n_1 = 0$, $n_2 = 2$, $n_3 = 2$, and $n_4 = 4$.

To test the ability of Scheme 2 to describe intra- and intersubunit cooperativity, we replotted the data from Figs. 2 and 4 in Fig. 5 A for the six different types of examined channels 4(RB), 2(RB)+2(ΔΔ), 2(ΔB)+2(RΔ), 4(RΔ), 4(ΔB), and 4(ΔΔ), and then simultaneously fitted all the data. The *Po* versus Ca^{2+} response for all these channel types was approximated by Scheme 2 (continuous lines, Fig. 5 A). The fitting was done with identical parameters for all channel types, except for the values of n, which were fixed by the stoichiometry of the Ca^{2+} sensors. The value of W, the empirical intrasubunit cooperativity factor, was 1.19, indicating positive cooperativity between the RCK1 sensor and the Ca bowl when they are on the same subunit.

(SCHEME 2)

$$Po = \frac{P\max}{1 + L(V)\left(\left(\left(\frac{1+[Ca]/K_{RC}}{1+[Ca]/K_{RO}}\right)\left(\frac{1+[Ca]/K_{BC}}{1+[Ca]/K_{BO}}\right)\right)^{W}\right)^{n1}\left(\frac{1+[Ca]/K_{RC}}{1+[Ca]/K_{RO}}\right)^{n2}\left(\frac{1+[Ca]/K_{BC}}{1+[Ca]/K_{BO}}\right)^{n3}\left(\frac{1+[Ca]/K_{MC}}{1+[Ca]/K_{MO}}\right)^{n4}}$$

The fitted equilibrium constants for the binding of Ca^{2+} to the RCK1 sensor and the Ca bowl were similar but not identical (see figure legend), giving rise to the three clustered lines for the 4(RΔ), 4(ΔB), and 2(ΔB)+2(RΔ) channels.

To explore further whether the intra- and intersubunit cooperativity in Scheme 2 is consistent with the gating of BK channels, we examined whether this equation could account for the Ca^{2+} activation of BK channels with different combinations of high-affinity Ca^{2+} sensors than those examined in Fig. 5 A. For these channels zero, one, two, three, or four of the subunits had their Ca-bowl sensors removed by mutation while keeping the RCK1 sensor and the low-affinity Ca^{2+}/Mg^{2+} sensor intact on each subunit. The data, which are from the study of Niu and Magleby (2002), are plotted in Fig. 5 B and show that the deletion of each Ca bowl leads to a step decrease in the Hill coefficient and a step decrease in K_d. The data in Fig. 5 B were simultaneously fitted with Scheme 2, where n_2 equals the number of subunits without a Ca bowl, $n_1 = (4 - n_2)$, $n_3 = 0$, and $n_4 = 4$. As shown in Fig. 5 B (continuous lines), Scheme 2 also described the decreasing Hill coefficients and shifts to higher apparent K_d as the number of subunits with Ca bowls was decreased from four to zero.

The dose–response curve for the 4(RΔ) channels in the study of Niu and Magleby (2002) was steeper and right shifted (Fig. 5 B, filled circles) compared with the 4(RΔ) channels in Fig. 5 A (blue squares). The steeper response in Fig. 5 B would be expected because the dose–response data for each channel of the same type was plotted after shifting the data for each individual channel to align the K_d to the average K_d for channels of the same type. Such shifting removes the variation in K_d that typically occurs among BK channels, leading to steeper slopes (discussed in Niu and Magleby, 2002). For Fig. 5 A, the data were averaged without shifting in order to obtain error bars and because of data at a limited number of $Ca^{2+}{}_i$ for some of the channels contributing to the averaged data, which did not allow determination of the individual K_d required for shifting. The right shift most likely reflects that different Ca-bowl mutations were used in the two studies, which can produce somewhat different effects (Schreiber and Salkoff, 1997; Bao et al., 2002). Consequently, the best-fitted parameters for Scheme 2 were somewhat different for the two studies.

Although Scheme 2 could approximate the *Po* vs. $Ca^{2+}{}_i$ response for a wide range of distribution and number of high-affinity Ca^{2+} sensors on the subunits (Fig. 5), the intrasubunit cooperativity factor *W* in this equation is an empirical parameter, and consequently, Scheme 2 becomes an empirical equation when *W* differs from 1.0. Furthermore, since both high-affinity Ca^{2+} sensors on the same subunit would not always have a bound Ca^{2+}, then the number of paired sensors is not given strictly by the number of subunits with two high-affinity Ca^{2+} sensors. This is currently incorporated into the fitted value of *W*, but an expanded version of Scheme 2 would be required to explicitly take this into account. Scheme 2, of course, is only one of many different schemes that could be proposed to incorporate intrasubunit cooperativity. For example, we also examined some models in which intrasubunit interactions occurred through changes in the binding affinities for the two high-affinity sensors rather than through the empirical *W* cooperativity factor. These models could also approximate the data but were more complex with a larger number of free parameters. Scheme 2 is a simple equilibrium model. Any actual physical model for cooperativity is likely to be more complex than Scheme 2. Nevertheless, Scheme 2 demonstrates that a model in which intrasubunit cooperativity is nested within intersubunit cooperativity can approximate the experimental data over a wide range of configurations of high-affinity Ca^{2+} binding sensors on the subunits.

DISCUSSION

Small changes in $Ca^{2+}{}_i$ can lead to large changes in the *Po* for BK channels (Barrett et al., 1982; McManus et al., 1985; Golowasch et al., 1986; Cui et al., 1997; Nimigean and Magleby, 1999; Bian et al., 2001). This highly cooperative activation involves at least three Ca^{2+} sensors per subunit. Two of these are high-affinity (μM) Ca^{2+} sensors defined by mutations to D362/D367 (RCK1 sensor) and to the Ca bowl, and the third is a low-affinity Ca^{2+}/Mg^{2+} sensor defined by mutations to E374/E399 (see INTRODUCTION). The objective of our study was to determine the contributions of the two high-affinity Ca^{2+} sensors to the cooperative activation of BK channels by Ca^{2+}. The approach was to examine BK channels with different configurations of the high-affinity Ca^{2+} sensors on the subunits. We found that the two high-affinity Ca^{2+} sensors contributed about equally to

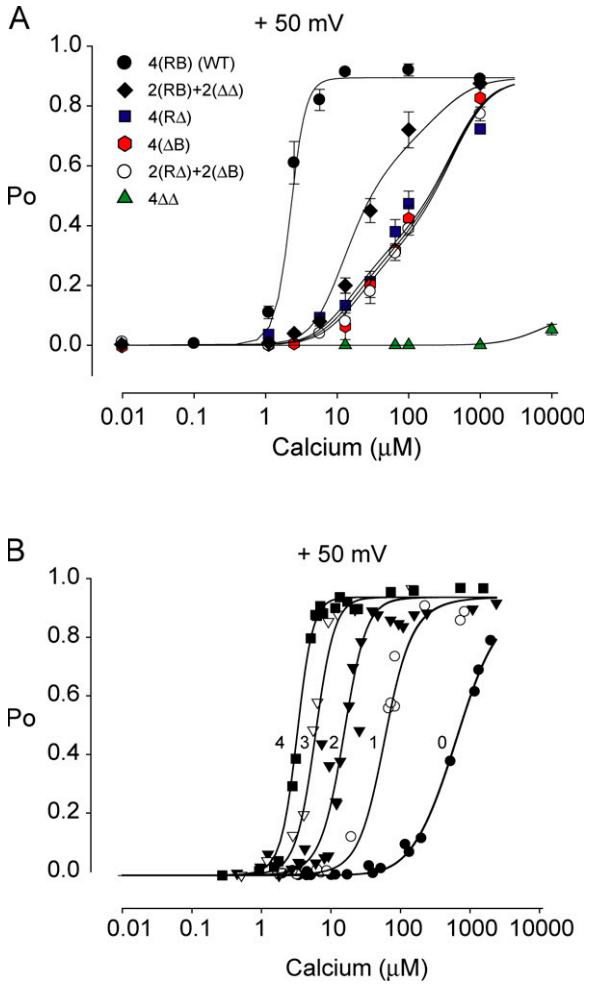

Figure 5. A gating model incorporating both intra- and intersubunit cooperativity (Scheme 2) can describe the Ca^{2+}-dependent activation of BK channels comprised of subunits with different numbers and distributions of high-affinity Ca^{2+} sensors. (A) *Po* vs. $Ca^{2+}{}_i$ plots for the six different channel types, as indicated. The continuous lines are simultaneous fits with Scheme 2 to all the plotted data and were calculated with $L(V) = 2500$ (from Niu and Magleby, 2002), $K_{BC} = 6.3$ μM, $K_{BO} = 1.0$ μM, $K_{RC} = 7.8$ μM, $K_{RO} = 1.3$ μM, $K_{MC} = 3000$ μM; $K_{MO} = 644$ μM, $W = 1.19$, $P_{max} = 0.90$. An assumption that the two high-affinity Ca^{2+} sites were identical gave an equally good fit (not shown) with $L(V) = 2500$, $K_{BC} = K_{RC} = 6.9$ μM, $K_{BO} = K_{RO} = 1.1$ μM, $K_{MC} = 3000$ μM, $K_{MO} = 644$ μM, $W = 1.19$. The values of n for each curve were set by the subunit composition (see text). K_{MC} was poorly defined and was set to the same value of both fits. (B) *Po* vs. $Ca^{2+}{}_i$ plots for the data from Niu and Magleby (2002) for BK channels with different numbers of Ca bowls. From left to right the subunit composition was 4(RB), 3(RB)+1(RΔ), 2(RB)+2(RΔ), 1(RB)+3(RΔ), and 4(RΔ). The continuous lines are simultaneous fits with Scheme 2 to all the data in part B, and were calculated with $L(V) = 2500$, $K_{BC} = 7.18$ μM, $K_{BO} = 1.00$ μM, $K_{RC} = 110.35$ μM, $K_{RO} = 18.98$ μM, $K_{MC} = 3000$ μM; $K_{MO} = 961$ μM, $W = 1.63$, and $P_{max} = 0.95$.

activating the channel when there was only one high-affinity Ca^{2+} sensor per subunit. We also found that two high-affinity Ca^{2+} sensors on the same subunit were much more effective in increasing open probability (*Po*) than when they were on separate subunits, indicating positive intrasubunit cooperativity. An empirical model incorporating intrasubunit cooperativity nested within intersubunit cooperativity could approximate the *Po* vs. Ca^{2+} response for eight possible subunit configurations of the high-affinity Ca^{2+} sensors, as well as three additional configurations from a previous study. The question then arises as to possible mechanisms for the intra- and intersubunit cooperativity.

Intrasubunit Cooperativity Appears To Be Nested within Intersubunit Cooperativity

Previous studies for the gating of BK channels have found that the Ca^{2+} activation of the channel could be described by assuming that each considered Ca^{2+} sensor acts independently but jointly to activate the channel (Cox and Aldrich, 2000; Cui and Aldrich, 2000; Shi and Cui, 2001; Zhang et al., 2001; Horrigan and Aldrich, 2002; Niu and Magleby, 2002; Xia et al., 2002). Such a model is described by Scheme 1 in which the affinity of each Ca^{2+} sensor is independent of Ca^{2+} binding at other sensors. In Scheme 1 the cooperativity arises from joint action of independent Ca^{2+} sensors on the gates.

To account for our observations that two high-affinity Ca^{2+} sensors on the same subunit are more effective in activation of the channel than when they are on separate subunits, we introduced an empirical intrasubunit cooperativity factor W in Scheme 2 that facilitates the ability of two high-affinity Ca^{2+} sensors on the same subunit to activate the channel. The physical basis for the intrasubunit cooperativity is not known but, in terms of Scheme 2, is consistent with the possibility that intersubunit cooperativity comes from the independent but joint action of each subunit to open the gates of the channel, with intrasubunit cooperativity facilitating the independent contribution of the individual subunits. Thus, intrasubunit cooperativity appears to be nested within intersubunit cooperativity. Suggestions of cooperative interactions that go beyond Scheme 1 have been inferred from previous studies (Cox et al., 1997; Rothberg and Magleby, 1999, 2000; Cui and Aldrich, 2000; Horrigan and Aldrich, 2002; Xia et al., 2002, 2004; Horrigan et al., 2005), so it is to be expected that Scheme 1 would need to be expanded.

Why BK channels have evolved such an elaborate mechanism for high-affinity Ca^{2+} activation that uses eight high-affinity sites of two different types is not clear but may reflect mechanical/energetic factors related to extracting sufficient energy from Ca^{2+} binding for Ca^{2+} activation of the channel over a wide range of both Ca^{2+} and voltage. $Mg^{2+}{}_i$ activates BK channels by binding to low-affinity sites and can also modulate BK channel activity through inhibitory action on the high-affinity sites (Shi and Cui, 2001; Zhang et al., 2001; Xia et al., 2002; Qian and Magleby, 2003; Kubokawa et al., 2005; Zeng et al., 2005). To what extent Mg^{2+} inhibition may act by

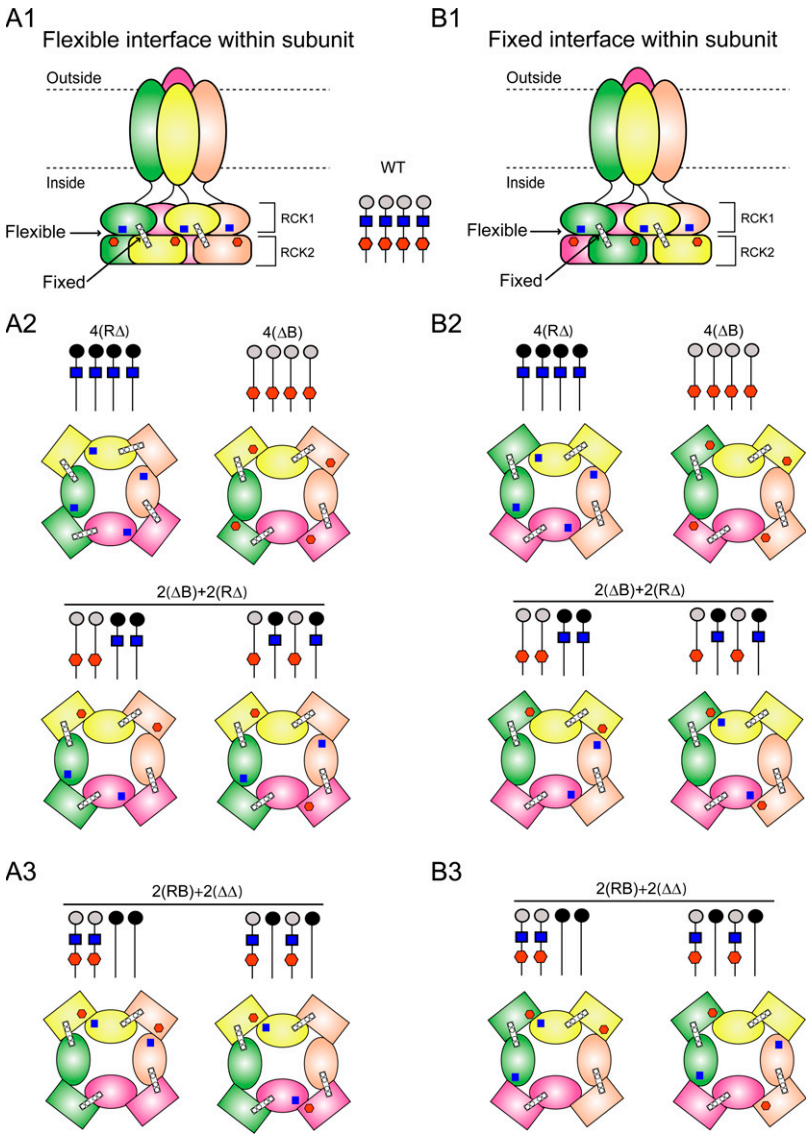

Figure 6. If the assumptions are made that the high-affinity Ca^{2+} sensors act at a flexible interface and that the interfaces between RCK domains in the gating ring alternate between fixed and flexible, then the data are consistent with a flexible, rather than a fixed, interface between the RCK1 and RCK2 domains of a single subunit. Schematic diagrams of WT BK channels and their gating rings are presented with different distributions of the high-affinity Ca^{2+} sensors assuming (A1–A3) a flexible intrasubunit interface or (B1–B3) a fixed intrasubunit interface. Transmembrane segments S0–S5 are removed in the side views of the BK channels in A1 and B1 to show the S6 gates. RCK1 domains are ellipses, RCK2 domains are squares, RCK1 sensors are blue squares, Ca bowls are red hexagons, RCK domains from the same subunit are of the same color, fixed interfaces are indicated by a bar across the interface, and flexible interfaces are indicated by contact between the RCK1 and RCK2 domains. The distributions of the RCK1 sensors and Ca bowls on the subunits are indicated in the stick diagrams for each channel type. The four channel types in A2 (for flexible intrasubunit interfaces) had similar Ca^{2+} response curves and required 3.9-fold more Ca^{2+} for half activation than the channel types in A3. These same channel types are repeated in B2 and B3 for fixed intrasubunit interfaces. The consistent distributions of high-affinity Ca^{2+} sensors in A2 and A3 assuming a flexible intrasubunit interface can be contrasted to the inconsistent distributions in B2 and B3 assuming a fixed intrasubunit interface, suggesting a flexible intrasubunit interface.

altering intrasubunit cooperativity between the two high-affinity sites will need to be investigated.

Possible Gating Ring Structures of BK Channels

To gain insight into possible mechanisms for intra- and intersubunit cooperativity, we now examine our findings in light of what is known about the structural basis for the Ca^{2+}-dependent gating of K^+ channels. It has been proposed, based on analogy to the crystal structure of a Ca^{2+}-modulated bacterial K^+ channel, MthK, that the intracellular COOH terminus of BK channels forms a large intracellular gating ring comprised of eight RCK (regulator of the conductance of K^+) domains (Jiang et al., 2001; Jiang et al., 2002). It has also been proposed that binding of Ca^{2+} to the gating ring may increase *Po* by expanding the gating ring to open the gates (Jiang et al., 2002; Niu et al., 2004; Dong et al., 2005). Based on these proposals, cartoons of hypothetical gating ring structures for WT BK channels are presented in Fig. 6. RCK1 and RCK2 domains are included in the cartoons based on the structure of MthK (Jiang et al., 2002), but it must be emphasized that these are assumed structures, as the actual structure of BK channels is unknown. It should also be noted that the RCK1 and RCK2 domains in MthK channels are identical, whereas the presumed RCK1 and RCK2 domains of BK channels have limited sequence identity. Nevertheless, for purposes of discussion, it will be assumed that BK channels have a gating ring comprised of RCK1 and RCK2 domains, similar to MthK.

With these assumptions it is not known whether the intrasubunit interface between the RCK1 and RCK2 domains in the assumed gating ring of BK channels is fixed or flexible (see below), so both types of configuration are shown: Fig. 6 A1 is drawn assuming a flexible interface between the RCK1 and RCK2 domains of each subunit, and Fig. 6 B1 is drawn assuming a fixed interface between the RCK1 and RCK2 domains of each

subunit (see below). Of the seven transmembrane segments of BK channels, S0–S5 are omitted in Fig. 6, A1 and B1, leaving only the S6 gates. The four RCK1 domains that are directly attached to the S6 gates by linkers form the upper part of the gating ring for the BK channels drawn in Fig. 6, A1 and B1, and the four RCK2 domains form the lower part of the gating ring (Jiang et al., 2001, 2002).

In MthK, there are a total of eight interfaces (contacts) between the eight RCK domains that alternate between fixed and flexible around the gating ring (Jiang et al., 2002), although the "fixed" interfaces may also have some flexibility (Dong et al., 2005). If BK channels have a gating ring similar to MthK channels, then BK channels would also have alternating fixed and flexible interfaces (Jiang et al., 2002). Consequently, alternating fixed interfaces (bars) and flexible interfaces (contacts) are shown in Fig. 6, A1 and B1. Notice that each interface, whether fixed or flexible, occurs between an RCK1 domain on the upper part of the gating ring and an RCK2 domain on the lower part of the gating ring. For BK channels, each proposed RCK2 domain would be attached to an RCK1 domain with a nonconserved RCK1–RCK2 linker (Schreiber and Salkoff, 1997; Schreiber et al., 1999). Neither the expression nor the function of BK channels requires that the RCK1–RCK2 linker be intact, as functional channels are obtained by injecting separate messenger RNA for the core (S0–S6 plus RCK1) and tail (RCK2) of the channel (Meera et al., 1997; Schreiber and Salkoff, 1997; Schreiber et al., 1999; Moss and Magleby, 2001; Qian et al., 2002; Schmalhofer et al., 2005). Because an intact RCK1–RCK2 linker is not required for function, RCK1–RCK2 linkers are not shown in Fig. 6.

Support for the gating ring model depicted in Fig. 6 (A1 and B1) comes from the observations that RCK domains isolated from MthK can form either dimers or octamers in solution depending on the ionic conditions, with comparison of crystal structures indicating movement at the flexible interfaces (Dong et al., 2005), although not as large as expected, suggesting that the "fixed" interfaces may also have some flexibility (Dong et al., 2005). Further support for a gating ring model for BK channels comes from the observations that shortening the linkers between the gating ring and the S6 gates increases *Po* and lengthening the linkers has the opposite effect, and this is the case over a wide range of Ca^{2+} (Niu et al., 2004).

Is the Intrasubunit Interface Fixed or Flexible?

When considering possible mechanisms for intra- and intersubunit cooperativity in BK channels, it would be most useful to know whether the interface formed between the proposed RCK1 and RCK2 domains on the same subunit is fixed or flexible. Analogy to MthK channels cannot be used to answer this question because the RCK2 domains of MthK channels are not directly attached to the RCK1 domains but are separate subunits assembled from solution (Jiang et al., 2002; Dong et al., 2005). Consequently, we explored if examination of our experimental data could give insight into whether the intrasubunit interfaces for BK channels were fixed or flexible.

Our approach was to compare the theoretical distributions of high-affinity Ca^{2+} sensors for assumed flexible or fixed intrasubunit interfaces to the Ca^{2+} response of the channels to determine whether either type of interface could be excluded because of inconsistency between the distributions of Ca^{2+} sensors and response. The locations of the high-affinity Ca^{2+} sensors on the gating ring are shown in Fig. 6 for the various configurations of channels considered in this paper. In Fig. 6 (A1–A3) the intrasubunit interfaces are assumed to be flexible and the intersubunit interfaces fixed. In Fig. 6 (B1–B3), the opposite configuration is assumed. Fig. 6 A1 and Fig. 6 B1 are side views of simplified WT channels, as discussed above, and A2–A3 and B2–B3 are schematic diagrams of only the gating ring looking into the channel from below. In these drawings RCK1 domains are ellipses, RCK2 domains are rectangles, RCK1 Ca^{2+} sensors are blue squares, Ca bowls are red hexagons, each fixed interface between RCK1 and RCK2 domains is indicated by a stabilizing bar across the interface, each flexible interface between RCK1 and RCK2 domains is indicated by contact between the two domains, and RCK1 and RCK2 domains from the same subunit are of the same color. For both flexible and fixed intrasubunit interfaces, it is expected that the $2(\Delta B)+2(R\Delta)$ channels and the $2(RB)+2(\Delta\Delta)$ channels will be expressed in two different assemblies: with the same type of subunit adjacent and with the same type of subunit diagonal. Consequently, both adjacent and diagonal configurations are presented, but it should be noted that the same conclusions would be reached if only the adjacent or the diagonal configurations were expressed. It will be argued in the sections below that our data are fully consistent with a flexible intrasubunit interface. The key assumptions in this analysis are that BK channels have a gating ring comprised of RCK domains, that the interfaces between the RCK domains alternate between fixed and flexible, and that the high-affinity Ca^{2+} sensors act at the flexible interfaces. These assumptions are based on analogy to the MthK channel, which has a gating ring comprised of RCK domains with alternating fixed and flexible interfaces, and the further observation that the binding of Ca^{2+} across the flexible interface of MthK channels induces the gating ring to expand (Jiang et al., 2002; Dong et al., 2005).

One High-affinity Ca^{2+} Sensor per Subunit. We found that channels with one high-affinity Ca^{2+} sensor per subunit, independent of whether the Ca^{2+} sensors were RCK1 sensors, Ca bowls, or a mixture of both, gave approximately

the same Po versus Ca^{2+} response (Fig. 1, B and C; Fig. 2, continuous line). The subunit locations of the high-affinity Ca^{2+} sensors for the four possible configurations of these functionally equivalent channels are presented in Fig. 6 A2 for an assumed flexible intrasubunit interface and in Fig. 6 B2 and for an assumed fixed intrasubunit interface. For an assumed flexible intrasubunit interface, each of the four configurations of the channel with one high-affinity Ca^{2+} sensor per subunit also had one high-affinity Ca^{2+} sensor per flexible interface (Fig. 6 A2). On this basis, each of the channels examined in Fig. 6 A2 gave the same Ca^{2+} response because each of the channels had a consistent distribution of one high-affinity Ca^{2+} sensor (either an RCK1 sensor or Ca bowl) per flexible interface.

In contrast, for an assumption of a fixed intrasubunit interface for one high-affinity Ca^{2+} sensor per subunit, there was an inconsistent distribution of Ca^{2+} sensors at the flexible interfaces (Fig. 6 B2). Two of the configurations (Fig. 6 B2, top row) had one Ca^{2+} sensor per flexible interface. Another configuration (Fig. 6 B2, bottom left) had two flexible interfaces with one Ca^{2+} sensor each, one flexible interface with two Ca^{2+} sensors, and one flexible interface with no Ca^{2+} sensors. The remaining configuration (Fig. 6 B2, bottom right) had two flexible interfaces with two Ca^{2+} sensors each and two flexible interfaces without Ca^{2+} sensors. Such diversity in the distribution of high-affinity Ca^{2+} sensors at the flexible interfaces of the channels in Fig. 6 B2 is inconsistent with the experimental observations that channels with one high-affinity Ca^{2+} sensor per subunit gave approximately the same response to Ca^{2+}. This inconsistency argues against a fixed intrasubunit interface.

Two High-affinity Ca^{2+} Sensors on Each of Two Subunits and No High-affinity Ca^{2+} Sensors on the Other Two Subunits. When the configuration of four high-affinity Ca^{2+} sensors per channel was two Ca^{2+} sensors on each of two subunits and no Ca^{2+} sensors on each of two subunits, as in Fig. 6 (A3 and B3), then the Ca^{2+} required to half activate the channel was decreased 3.9-fold (Fig. 4). Hence, two high-affinity Ca^{2+} sensors on each of two subunits were much more effective than when there was one Ca^{2+} sensor on each of four separate subunits. For an assumption of a flexible intrasubunit interface (Fig. 6 A3), each of the two configurations of the channel with two Ca^{2+} sensors on each of two subunits and no Ca^{2+} sensors on each of two subunits would have two Ca^{2+} sensors at each of two flexible interfaces and no Ca^{2+} sensors at the other two flexible interfaces. Thus, the same Ca^{2+} response for both configurations in Fig. 6 A3 would be expected if the response depended on the distribution of paired Ca^{2+} sensors at the flexible interfaces and not on whether identical subunits were adjacent or diagonal.

For an assumption of a fixed intrasubunit interface (Fig. 6 B3), one of the configurations of channels with two Ca^{2+} sensors on each of two subunits and no Ca^{2+} sensors on each of two subunits would have two Ca^{2+} sensors at one flexible interface, one Ca^{2+} sensor at each of two flexible interfaces, and no Ca^{2+} sensors at one flexible interface (Fig. 6 B3, left). The other configuration would have one Ca^{2+} sensor at each of the four flexible interfaces (Fig. 6 B3, right). Such a pronounced difference in the distribution of high-affinity Ca^{2+} sensors at the flexible interfaces of the two possible channel configurations in Fig. 6 B3 might be expected to produce a large difference in response. Yet, there was no indication that this was the case. Furthermore, both of the channel configurations in Fig. 6 B3 are essentially equivalent to channel configurations in Fig. 6 B2, yet the channels for Fig. 6 B3 required 3.9-fold less Ca^{2+} for half activation than those in Fig. 6 B2. These inconsistencies between the distributions of the Ca^{2+} sensors and the Ca^{2+} responses for an assumed fixed intrasubunit interface (Fig. 6, B2 and B3) are in marked contrast to the consistent relationships observed for an assumed flexible intrasubunit interface (Fig. 6, A2–A3). Consequently, the data suggest a flexible intrasubunit interface for BK channels, and such an interface will be assumed for further discussion of mechanism. It should be emphasized that this conclusion is based on the assumptions that BK channels have a gating ring comprised of RCK domains similar to MthK channels, that the interfaces between RCK1 and RCK2 domains alternate between fixed and flexible, and that the high-affinity Ca^{2+} sensors act at the flexible interfaces. Alternatively, if the interfaces do not alternate between fixed and flexible, or if the Ca^{2+} sensors act at the fixed interfaces (although it would be difficult to see how Ca^{2+} sensors could have any action at a fixed interface or have cooperative interactions across a fixed interface), then the conclusion would have been just the opposite.

Possible Mechanisms for Intrasubunit Cooperativity

We observed that two high-affinity Ca^{2+} sensors on the same subunit were much more effective in activating the channel then when on separate subunits (Fig. 4), indicating intrasubunit cooperativity. If the interface between RCK1 and RCK2 domains on the same subunit is flexible, as considered above, then taken together, these observations indicate that two high-affinity Ca^{2+} sensors acting on either side of a flexible intrasubunit interface are far more effective at opening the channel than two high-affinity Ca^{2+} sensors located singly on separate subunits, giving the conditions for intrasubunit cooperativity.

Scheme 2, which incorporates intrasubunit cooperativity nested within intersubunit cooperativity, could approximate the Ca^{2+} response of the different examined

configurations of the high-affinity Ca^{2+} sensors on the subunits. In terms of the diagrams of the gating rings in Fig. 6 (A1–A3), intersubunit cooperativity would arise from independent but joint action of the Ca^{2+} sensors on different subunits to expand the gating ring and open the channel, whereas intrasubunit cooperativity would arise from cooperative action of Ca^{2+} sensors located on either side of the flexible interface of a single subunit, leading to a more effective expansion of the gating ring than if the Ca^{2+} sensors were located on different subunits. The molecular machinery in BK channels that makes two Ca^{2+} sensors on the same subunit more effective than two Ca^{2+} sensors on separate subunits is unknown, but for MthK channels, the two Ca^{2+} binding sites located across each flexible interface are separated by only 11 Å (Dong et al., 2005), such that expansion of the interface induced by Ca^{2+} binding at one site might be expected to influence the neighboring Ca^{2+} binding site.

Whereas the Ca bowl and the RCK1 sensors are both of high affinity with similar effects on the *Po* vs. Ca^{2+} response in our relatively low resolution experiments, these sites are not identical, as they have differential cation sensitivity, somewhat different K_d, and differential effects on the activation and deactivation properties of the channel (Schreiber and Salkoff, 1997; Bao et al., 2002; Xia et al., 2002; Zeng et al., 2005). Furthermore, whereas the RCK1 and RCK2 domains of MthK are essentially identical, the proposed RCK1 and RCK2 domains of BK channels have only very limited sequence identity, and the Ca bowl appears as an additional structure downstream of the proposed RCK2 domain (Schreiber and Salkoff, 1997; Schreiber et al., 1999; Bian et al., 2001; Jiang et al., 2001). Thus, it is expected that the locations of the high-affinity Ca^{2+} binding sites in BK channels will differ from the symmetrical structure of the low-affinity Ca^{2+} binding sites in MthK. Consequently, whereas Scheme 2 and the schematic diagrams of the BK channel in Fig. 6 (which are based on an assumed structure) can serve to summarize the data and should be useful for designing future experiments, the actual structure is likely to differ significantly from the structure assumed for purposes of discussion, and it is also anticipated that the gating mechanism will be more complex than Scheme 2.

Cooperativity in Other Channels

Various types of intersubunit cooperativity have been described previously. For example, glycine receptors comprised of homomeric α1 subunits can bind a glycine molecule on each of five subunits, with interaction between the binding sites when the channel is still closed, giving intersubunit cooperativity before the conformational change associated with channel opening (Beato et al., 2004). For NMDA receptors, a steric interaction exists between NR1 and NR2 subunits that modulates glycine affinity (Regalado et al., 2001). For voltage-gated potassium channels, the S4 voltage sensors can first move independently and then move cooperatively to open the channel (Smith-Maxwell et al., 1998a,b; Schoppa and Sigworth, 1998a,b,c; Ledwell and Aldrich, 1999; Patlak, 1999; Mannuzzu and Isacoff, 2000; Pathak et al., 2005; Tombola et al., 2005). The voltage sensors in BK channels act mainly independently but jointly to open the gates (Horrigan and Aldrich, 1999, 2002; Horrigan et al., 1999; Cox and Aldrich, 2000). For cyclic nucleotide-gated channels, it has been proposed that the four subunits may associate and activate as two independent dimers with independent binding of ligand to each subunit that forms a dimer, but the conformational changes of the two subunits within the dimer upon ligand binding can be cooperative and concerted (Liu et al., 1998; Richards and Gordon, 2000; Craven et al., 2006). For the above examples of intersubunit cooperativity, there are two general types of mechanisms: cooperativity arising from independent but joint action of the subunits to open the gates and cooperativity arising from interactions among the binding sites or subunits.

BK channels may also have these two types of cooperative action, with intrasubunit cooperativity being a likely candidate for interactions among the high-affinity Ca^{2+} sensors located on the same subunit, and intersubunit cooperativity arising from independent but joint action of high-affinity Ca^{2+} sensors on different subunits. We found that two high-affinity Ca^{2+} sensors on a single subunit were much more effective at activating the channel than two high-affinity Ca^{2+} sensors on separate subunits, indicating positive intrasubunit cooperativity. A model with intrasubunit cooperativity nested within intersubunit cooperativity was consistent with the experimental observations.

Supported in part by grants from the National Institutes of Health (AR32805) and the Muscular Dystrophy Association.

Olaf S. Andersen served as editor.

Submitted: 3 January 2006
Accepted: 13 September 2006

REFERENCES

Adelman, J.P., K.Z. Shen, M.P. Kavanaugh, R.A. Warren, Y.N. Wu, A. Lagrutta, C.T. Bond, and R.A. North. 1992. Calcium-activated potassium channels expressed from cloned complementary DNAs. *Neuron.* 9:209–216.

Atkinson, N.S., G.A. Robertson, and B. Ganetzky. 1991. A component of calcium-activated potassium channels encoded by the *Drosophila* slo locus. *Science.* 253:551–555.

Bao, L., A.M. Rapin, E.C. Holmstrand, and D.H. Cox. 2002. Elimination of the BK(Ca) channel's high-affinity Ca^{2+} sensitivity. *J. Gen. Physiol.* 120:173–189.

Barrett, J.N., K.L. Magleby, and B.S. Pallotta. 1982. Properties of single calcium-activated potassium channels in cultured rat muscle. *J. Physiol.* 331:211–230.

Beato, M., P.J. Groot-Kormelink, D. Colquhoun, and L.G. Sivilotti. 2004. The activation mechanism of α1 homomeric glycine receptors. *J. Neurosci.* 24:895–906.

Bian, S., I. Favre, and E. Moczydlowski. 2001. Ca^{2+}-binding activity of a COOH-terminal fragment of the *Drosophila* BK channel involved in Ca^{2+}-dependent activation. *Proc. Natl. Acad. Sci. USA.* 98:4776–4781.

Brenner, R., G.J. Perez, A.D. Bonev, D.M. Eckman, J.C. Kosek, S.W. Wiler, A.J. Patterson, M.T. Nelson, and R.W. Aldrich. 2000. Vasoregulation by the β1 subunit of the calcium-activated potassium channel. *Nature.* 407:870–876.

Butler, A., S. Tsunoda, D.P. McCobb, A. Wei, and L. Salkoff. 1993. mSlo, a complex mouse gene encoding "maxi" calcium-activated potassium channels. *Science.* 261:221–224.

Cox, D.H., and R.W. Aldrich. 2000. Role of the β1 subunit in large-conductance Ca^{2+}-activated K^+ channel gating energetics. Mechanisms of enhanced Ca^{2+} sensitivity. *J. Gen. Physiol.* 116:411–432.

Cox, D.H., J. Cui, and R.W. Aldrich. 1997. Allosteric gating of a large conductance Ca-activated K^+ channel. *J. Gen. Physiol.* 110:257–281.

Craven, K.B., and W.N. Zagotta. 2006. CNG and HCN channels: two peas, one pod. *Annu. Rev. Physiol.* 68:10.1–10.27.

Cui, J., and R.W. Aldrich. 2000. Allosteric linkage between voltage and Ca^{2+}-dependent activation of BK-type mslo1 K^+ channels. *Biochemistry.* 39:15612–15619.

Cui, J., D.H. Cox, and R.W. Aldrich. 1997. Intrinsic voltage dependence and Ca^{2+} regulation of mslo large conductance Ca-activated K^+ channels. *J. Gen. Physiol.* 109:647–673.

Diaz, L., P. Meera, J. Amigo, E. Stefani, O. Alvarez, L. Toro, and R. Latorre. 1998. Role of the S4 segment in a voltage-dependent calcium-sensitive potassium (hSlo) channel. *J. Biol. Chem.* 273:32430–32436.

Dong, J., N. Shi, I. Berke, L. Chen, and Y. Jiang. 2005. Structures of the MTHK RCK domain and the effect of Ca^{2+} on gating ring stability. *J. Biol. Chem.* 280:41716–41724.

Doyle, D.A., C.J. Morais, R.A. Pfuetzner, A. Kuo, J.M. Gulbis, S.L. Cohen, B.T. Chait, and R. Mackinnon. 1998. The structure of the potassium channel: molecular basis of K^+ conduction and selectivity. *Science.* 280:69–77.

Golowasch, J., A. Kirkwood, and C. Miller. 1986. Allosteric effects of Mg^{2+} on the gating of Ca^{2+}-activated K^+ channels from mammalian skeletal muscle. *J. Exp. Biol.* 124:5–13.

Hamill, O.P., A. Marty, E. Neher, B. Sakmann, and F.J. Sigworth. 1981. Improved patch-clamp techniques for high-resolution current recording from cells and cell-free membrane patches. *Pflugers Arch.* 391:85–100.

Horrigan, F.T., and R.W. Aldrich. 1999. Allosteric voltage gating of potassium channels II. Mslo channel gating charge movement in the absence of Ca^{2+}. *J. Gen. Physiol.* 114:305–336.

Horrigan, F.T., and R.W. Aldrich. 2002. Coupling between voltage sensor activation, Ca^{2+} binding and channel opening in large conductance (BK) potassium channels. *J. Gen. Physiol.* 120:267–305.

Horrigan, F.T., J. Cui, and R.W. Aldrich. 1999. Allosteric voltage gating of potassium channels I. Mslo ionic currents in the absence of Ca^{2+}. *J. Gen. Physiol.* 114:277–304.

Horrigan, F.T., S.H. Heinemann, and T. Hoshi. 2005. Heme regulates allosteric activation of the Slo1 BK channel. *J. Gen. Physiol.* 126:7–21.

Hu, L., J. Shi, Z. Ma, G. Krishnamoorthy, F. Sieling, G. Zhang, F.T. Horrigan, and J. Cui. 2003. Participation of the S4 voltage sensor in the Mg^{2+}-dependent activation of large conductance (BK) K^+ channels. *Proc. Natl. Acad. Sci. USA.* 100:10488–10493.

Jiang, Y., A. Lee, J. Chen, M. Cadene, B.T. Chait, and R. Mackinnon. 2002. Crystal structure and mechanism of a calcium-gated potassium channel. *Nature.* 417:515–522.

Jiang, Y., A. Pico, M. Cadene, B.T. Chait, and R. Mackinnon. 2001. Structure of the RCK domain from the *E. coli* K^+ channel and demonstration of its presence in the human BK channel. *Neuron.* 29:593–601.

Kaczorowski, G.J., H.G. Knaus, R.J. Leonard, O.B. McManus, and M.L. Garcia. 1996. High-conductance calcium-activated potassium channels; structure, pharmacology, and function. *J. Bioenerg. Biomembr.* 28:255–267.

Langton, P.D., M.T. Nelson, Y. Huang, and N.B. Standen. 1991. Block of calcium-activated potassium channels in mammalian arterial myocytes by tetraethylammonium ions. *Am. J. Physiol.* 260: H927–H934.

Ledwell, J.L., and R.W. Aldrich. 1999. Mutations in the S4 region isolate the final voltage-dependent cooperative step in potassium channel activation. *J. Gen. Physiol.* 113:389–414.

Liu, D.T., G.R. Tibbs, P. Paoletti, and S.A. Siegelbaum. 1998. Constraining ligand-binding site stoichiometry suggests that a cyclic nucleotide-gated channel is composed of two functional dimers. *Neuron.* 21:235–248.

Magleby, K.L. 2003. Gating mechanism of BK (Slo1) channels: so near, yet so far. *J. Gen. Physiol.* 121:81–96.

Mannuzzu, L.M., and E.Y. Isacoff. 2000. Independence and cooperativity in rearrangements of a potassium channel voltage sensor revealed by single subunit fluorescence. *J. Gen. Physiol.* 115:257–268.

McManus, O.B., A.L. Blatz, and K.L. Magleby. 1985. Inverse relationship of the durations of adjacent open and shut intervals for Cl and K channels. *Nature.* 317:625–627.

McManus, O.B., A.L. Blatz, and K.L. Magleby. 1987. Sampling, log binning, fitting, and plotting durations of open and shut intervals from single channels and the effects of noise. *Pflugers Arch.* 410:530–553.

McManus, O.B., L.M. Helms, L. Pallanck, B. Ganetzky, R. Swanson, and R.J. Leonard. 1995. Functional role of the β subunit of high conductance calcium-activated potassium channels. *Neuron.* 14:645–650.

McManus, O.B., and K.L. Magleby. 1988. Kinetic states and modes of single large-conductance calcium-activated potassium channels in cultured rat skeletal muscle. *J. Physiol.* 402:79–120.

Meera, P., M. Wallner, M. Song, and L. Toro. 1997. Large conductance voltage- and calcium-dependent K^+ channel, a distinct member of voltage-dependent ion channels with seven N-terminal transmembrane segments (S0-S6), an extracellular N terminus, and an intracellular (S9-S10) C terminus. *Proc. Natl. Acad. Sci. USA.* 94:14066–14071.

Moss, B.L., and K.L. Magleby. 2001. Gating and conductance properties of BK channels are modulated by the S9-S10 tail domain of the α subunit. A study of mSlo1 and mSlo3 wild-type and chimeric channels. *J. Gen. Physiol.* 118:711–734.

Nimigean, C.M., and K.L. Magleby. 1999. The β subunit increases the Ca^{2+} sensitivity of large conductance Ca^{2+}-activated potassium channels by retaining the gating in the bursting states. *J. Gen. Physiol.* 113:425–440.

Nimigean, C.M., and K.L. Magleby. 2000. Functional coupling of the β1 subunit to the large conductance Ca^{2+}-activated K^+ channel in the absence of Ca^{2+}. Increased Ca^{2+} sensitivity from a Ca^{2+}-independent mechanism. *J. Gen. Physiol.* 115:719–736.

Niu, X., and K.L. Magleby. 2002. Stepwise contribution of each subunit to the cooperative activation of BK channels by Ca^{2+}. *Proc. Natl. Acad. Sci. USA.* 99:11441–11446.

Niu, X., X. Qian, and K.L. Magleby. 2004. Linker-gating ring complex as passive spring and Ca^{2+}-dependent machine for a voltage- and Ca^{2+}-activated potassium channel. *Neuron.* 42:745–756.

Pallanck, L., and B. Ganetzky. 1994. Cloning and characterization of human and mouse homologs of the *Drosophila* calcium-activated potassium channel gene, slowpoke. *Hum. Mol. Genet.* 3:1239–1243.

Pathak, M., L. Kurtz, F. Tombola, and E. Isacoff. 2005. The cooperative voltage sensor motion that gates a potassium channel. *J. Gen. Physiol.* 125:57–69.

Patlak, J.B. 1999. Cooperating to unlock the voltage-dependent K channel. *J. Gen. Physiol.* 113:385–388.

Petkov, G.V., A.D. Bonev, T.J. Heppner, R. Brenner, R.W. Aldrich, and M.T. Nelson. 2001. β1-subunit of the Ca^{2+}-activated K^+ channel regulates contractile activity of mouse urinary bladder smooth muscle. *J. Physiol.* 537:443–452.

Qian, X., and K.L. Magleby. 2003. β1 subunits facilitate gating of BK channels by acting through the Ca^{2+}, but not the Mg^{2+}, activating mechanisms. *Proc. Natl. Acad. Sci. USA.* 100:10061–10066.

Qian, X., C.M. Nimigean, X. Niu, B.L. Moss, and K.L. Magleby. 2002. Slo1 tail domains, but not the Ca^{2+} bowl, are required for the β1 subunit to increase the apparent Ca^{2+} sensitivity of BK channels. *J. Gen. Physiol.* 120:829–843.

Regalado, M.P., A. Villarroel, and J. Lerma. 2001. Intersubunit cooperativity in the NMDA receptor. *Neuron.* 32:1085–1096.

Richards, M.J., and S.E. Gordon. 2000. Cooperativity and cooperation in cyclic nucleotide-gated ion channels. *Biochemistry.* 39:14003–14011.

Robitaille, R., M.L. Garcia, G.J. Kaczorowski, and M.P. Charlton. 1993. Functional colocalization of calcium and calcium-gated potassium channels in control of transmitter release. *Neuron.* 11:645–655.

Rothberg, B.S., and K.L. Magleby. 1999. Gating kinetics of single large-conductance Ca^{2+}-activated K^+ channels in high Ca^{2+} suggest a two-tiered allosteric gating mechanism. *J. Gen. Physiol.* 114:93–124.

Rothberg, B.S., and K.L. Magleby. 2000. Voltage and Ca^{2+} activation of single large-conductance Ca^{2+}-activated K^+ channels described by a two-tiered allosteric gating mechanism. *J. Gen. Physiol.* 116:75–99.

Schmalhofer, W.A., M. Sanchez, G. Dai, A. Dewan, L. Secades, M. Hanner, H.G. Knaus, O.B. McManus, M. Kohler, G.J. Kaczorowski, and M.L. Garcia. 2005. Role of the C-terminus of the high-conductance calcium-activated potassium channel in channel structure and function. *Biochemistry.* 44:10135–10144.

Schoppa, N.E., and F.J. Sigworth. 1998a. Activation of shaker potassium channels. I. Characterization of voltage-dependent transitions. *J. Gen. Physiol.* 111:271–294.

Schoppa, N.E., and F.J. Sigworth. 1998b. Activation of Shaker potassium channels. II. Kinetics of the V2 mutant channel. *J. Gen. Physiol.* 111:295–311.

Schoppa, N.E., and F.J. Sigworth. 1998c. Activation of Shaker potassium channels. III. An activation gating model for wild-type and V2 mutant channels. *J. Gen. Physiol.* 111:313–342.

Schreiber, M., and L. Salkoff. 1997. A novel calcium-sensing domain in the BK channel. *Biophys. J.* 73:1355–1363.

Schreiber, M., A. Yuan, and L. Salkoff. 1999. Transplantable sites confer calcium sensitivity to BK channels. *Nat. Neurosci.* 2:416–421.

Shen, K.Z., A. Lagrutta, N.W. Davies, N.B. Standen, J.P. Adelman, and R.A. North. 1994. Tetraethylammonium block of Slowpoke calcium-activated potassium channels expressed in *Xenopus* oocytes: evidence for tetrameric channel formation. *Pflugers Arch.* 426:440–445.

Shi, J., and J. Cui. 2001. Intracellular Mg^{2+} enhances the function of BK-type Ca^{2+}-activated K^+ channels. *J. Gen. Physiol.* 118:589–606.

Shi, J., G. Krishnamoorthy, Y. Yang, L. Hu, N. Chaturvedi, D. Harilal, J. Qin, and J. Cui. 2002. Mechanism of magnesium activation of calcium-activated potassium channels. *Nature.* 418:876–880.

Smith-Maxwell, C.J., J.L. Ledwell, and R.W. Aldrich. 1998a. Role of the S4 in cooperativity of voltage-dependent potassium channel activation. *J. Gen. Physiol.* 111:399–420.

Smith-Maxwell, C.J., J.L. Ledwell, and R.W. Aldrich. 1998b. Uncharged S4 residues and cooperativity in voltage-dependent potassium channel activation. *J. Gen. Physiol.* 111:421–439.

Kubokawa, M., Y. Sohma, J. Hirano, K.N. Makamura, and T. Kubota. 2005. Intracellular Mg^{2+} influences both open and closed times of a native Ca^{2+}-activated BK channel in cultured human renal proximal tubule cells. *J. Membr. Biol.* 207:69–89.

Tian, L., L.S. Coghill, H. McClafferty, S.H.-F. MacDonald, F.A. Antoni, P. Ruth, H.-G. Knaus, and M.J. Shipston. 2004. Distinct stoichiometry of BKCa channel tetramer phosphorylation specifies channel activation and inhibition by cAMP-dependent protein kinase. *Proc. Natl. Acad. Sci. USA.* 101:11897–11902.

Tombola, F., M.M. Pathak, and E.Y. Isacoff. 2005. Voltage-sensing arginines in a potassium channel permeate and occlude cation-selective pores. *Neuron.* 45:379–388.

Wang, Z.W., O. Saifee, M.L. Nonet, and L. Salkoff. 2001. SLO-1 potassium channels control quantal content of neurotransmitter release at the *C. elegans* neuromuscular junction. *Neuron.* 32:867–881.

Xia, X.M., X. Zeng, and C.J. Lingle. 2002. Multiple regulatory sites in large-conductance calcium-activated potassium channels. *Nature.* 418:880–884.

Xia, X.M., X. Zhang, and C.J. Lingle. 2004. Ligand-dependent activation of Slo family channels is defined by interchangeable cytosolic domains. *J. Neurosci.* 24:5585–5591.

Xu, J.W., and M.M. Slaughter. 2005. Large-conductance calcium-activated potassium channels facilitate transmitter release in salamander rod synapse. *J. Neurosci.* 25:7660–7668.

Zeng, X.H., X.M. Xia, and C.J. Lingle. 2005. Divalent cation sensitivity of BK channel activation supports the existence of three distinct binding sites. *J. Gen. Physiol.* 125:273–286.

Zhang, X., C.R. Solaro, and C.J. Lingle. 2001. Allosteric regulation of BK channel gating by Ca^{2+} and Mg^{2+} through a nonselective, low-affinity divalent cation site. *J. Gen. Physiol.* 118:607–636.